



Dynamically resolved self-assembly of S-layer proteins on solid surfaces

Journal:	<i>ChemComm</i>
Manuscript ID	CC-COM-06-2018-004597.R2
Article Type:	Communication

SCHOLARONE™
Manuscripts

Chemical Communications

Guidelines for referees



ChemComm is a forum for urgent high quality communications from across the chemical sciences.

Communications in *ChemComm* should be preliminary accounts of **original and urgent work** of significance to a general chemistry audience. The 2016 impact factor for *ChemComm* is **6.319**.

Only work within the top 25% of the field in terms of quality and interest should be recommended for publication. Acceptance should only be recommended if the content is of such **urgency and significant general interest** that rapid publication will be advantageous to the progress of chemical research.

Routine and incremental work – however competently researched and reported – should not be recommended for publication.

Articles which rely excessively on supplementary information should not be recommended for publication.

Thank you very much for your assistance in evaluating this manuscript.

General Guidance

Referees have the responsibility to treat the manuscript as confidential. Please be aware of our [Ethical Guidelines](#), which contain full information on the responsibilities of referees and authors, and our [Refereeing Procedure and Policy](#).

Supporting information and characterisation of new compounds

Experimental information must be provided to enable other researchers to reproduce the work accurately. It is the responsibility of authors to provide fully convincing evidence for the homogeneity, purity and identity of all compounds they claim as new. This evidence is required to establish that the properties and constants reported are those of the compound with the new structure claimed.

Please assess the evidence presented in support of the claims made by the authors and comment on whether adequate supporting information has been provided to address the above. Further details on the requirements for characterisation criteria can be found [here](#).

When preparing your report, please:

- comment on the originality, significance, impact and scientific reliability of the work;
- state clearly whether you would like to see the article accepted or rejected and give detailed comments (with references, as appropriate) that will both help the Editor to make a decision on the article and the authors to improve it;
- it is the expectation that only work with two strong endorsements will be accepted for publication.

Please inform the Editor if:

- there is a conflict of interest;
- there is a significant part of the work which you are not able to referee with confidence;
- the work, or a significant part of the work, has previously been published;
- you believe the work, or a significant part of the work, is currently submitted elsewhere;
- the work represents part of an unduly fragmented investigation.

Submit your report at <http://mc.manuscriptcentral.com/chemcomm>



Journal Name

COMMUNICATION

Dynamically resolved self-assembly of S-layer proteins on solid surfaces

Received 00th January 20xx,
Accepted 00th January 20xx

Bart Stel,^{a,b} Fernando Cometto,^a Behzad Rad,^c James J. De Yoreo^{*d} and Magalí Lingenfelder^{*a,b}

DOI: 10.1039/x0xx00000x

www.rsc.org/

By using high-speed and high-resolution Atomic Force Microscopy (AFM), it was possible to resolve within a single experiment the kinetic pathway in S-layer self-assembly at the solid-liquid interface, obtaining a model that accounts for the nucleation, growth and structural rearrangements in 2D protein self assembly across time (second to hours) and spatial scales (nm to microns).

Bacterial Surface Layers (S-layers) are two-dimensional crystalline protein layers that make up the outer cell membrane of many Gram-positive and Gram-negative bacteria and almost all archaea.^{1,2} S-layers are composed of individual proteins, which self-assemble into regularly ordered lattices that can have symmetries ranging from oblique (P1, P2) to square (P4) to hexagonal (P3, P6), depending on the proteins of the originating organism.^{3,4} The fact that S-layer proteins are the most abundant molecules in their respective organisms, points to a significant biological importance. Although no single function is found to be applicable to all instances of S-layer expressing organisms, structural integrity, permeability of the cell envelope and cell adhesion have all been related to the presence of S-layers.⁵

S-layer proteins can be purified and recrystallized into 2D lattices *ex vivo*, which enables their use in a wide range of applications. They are used as templates that drive the ordered adhesion of nanoparticles,^{6–8} immobilization matrices for functional biomolecules,^{9–12} adsorption matrices for metal ions^{13,14} and even as coatings that inhibit the adhesion of cells.¹⁵

The self-assembly of S-layer proteins on solid surfaces follows a non-classical multi-stage crystallization pathway (Figure 1).¹⁶ The actual crystallization of the individual proteins is preceded by a distinct condensation step that generates amorphous “globules”. Once formed, the crystalline S-layer is self-catalyzing and subsequent growth happens through the direct attachment of monomers. Furthermore, existing crystals never disappear,¹⁷ regardless of size, indicating that there is no bi-directional exchange between the crystalline S-layers and the SbpA protein (from *Lysinibacillus sphaericus*) monomers in solution. For this reason, Classical Nucleation Theory (CNT) cannot be applied here.¹⁸

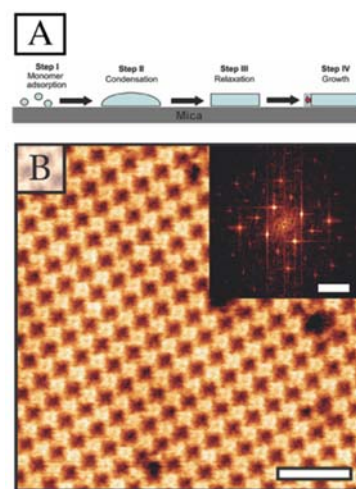


Figure 1 – S-layer self-assembly at the solid-liquid interface. (a) The formation of S-layer self-assembly on mica goes through four distinct steps: adsorption, condensation, relaxation and, finally, growth. (b) *In situ* AFM image showing that *ex vivo* recrystallization of S-layers on mica reproduces the native P4 symmetric structure. The tetrameric structure of the S-layer unit cell is clearly visible in the inset (FFT). Scale bars: 40 nm and 0.12 nm⁻¹ for the AFM image and the FFT image, respectively.

^a Max Planck-EPFL Laboratory for Molecular Nanoscience, École Polytechnique Fédérale de Lausanne, Switzerland.

magali.lingenfelder@epfl.ch

^b Institut de Physique, Ecole Polytechnique Fédérale de Lausanne, Switzerland.

^c Molecular Foundry, Lawrence Berkeley National Laboratory, Berkeley, California, USA.

^d Pacific Northwest National Laboratory, 902 Battelle Boulevard, Richland, Washington, 99354, USA. Department of Materials Science and Engineering, University of Washington, 302 Roberts Hall, Seattle, Washington, 98195, USA. James.De.Yoreo@pnnl.gov

The formation of stable ordered domains of S-layer proteins (SbpA) on mica is especially interesting because it combines three different dynamical processes. First, protein monomers adsorb to the solid-liquid interface, second, the adsorbed monomers undergo self-assembly, and finally, some of the self-assembled S-layers undergo a conformational change from a low conformation into a high conformation.^{16,19}

The different time scales of each process make it challenging to observe all the dynamic processes in one single experiment, i.e. the adsorption of SbpA to the mica-liquid interface takes place within minutes,¹⁶ whereas the conformational change of the fully formed S-layer crystals can take several hours.¹⁹ This experimental challenge can be overcome by using the high resolution and fast scanning speeds of a Dimension FastScan AFM system (Bruker Inc), in combination with a continuous flow through an *in situ* flow cell. The main advantage of the dynamic flow setup is that the concentration of monomers remain constant during the entire process, from seconds to hours. Moreover, the system can be observed at length scales ranging from molecular resolution until 30 μm . This enables the detailed tracking of all three processes in a single experiment. In order to start the tracking from the single proteins, the SbpA monomer was purified as described earlier.^{17,20} The mica-liquid interface was continuously imaged while a 20 $\mu\text{l/s}$ liquid flow is changed from pure buffer solution to a buffer solution containing SbpA monomers at 50 $\mu\text{g/ml}$. Representative snapshots of the whole process are shown in Figure 2.

We observe that crystallization to form the 2D layer starts few minutes after protein absorption, and structural changes from

low to high conformations (visualized as dark vs bright protrusions in Figure 2) also start to occur at an early stage, becoming dominant after ~ 70 min.

This new information allows us to modify the kinetic models previously reported by Chung et al.¹⁶ and Shin et al.¹⁹ and combine them into a single model, which accurately describes both S-layer formation and subsequent conformational change. Chung et al. studied the self-assembly of S-layers on supported lipid bilayers (SLBs) and accurately predicted the S-layer island size over time by using a perimeter driven growth model. This model defines the growth of an S-layer island as the number of tetrameric unit cells that is added per unit time, i.e. dN_T/dt . The growth is linearly proportional to the number of available unit cells along its border, $\sqrt{N_T}$, and an experimentally determined tetramer attachment rate, R , i.e. $dN_T/dt \sim \sqrt{N_T} \cdot R$. Under their specific experimental conditions, the nucleation and growth of the S-layer crystals did not overlap, i.e. no nucleation was observed once S-layer crystals had formed at the solid-liquid interface. Furthermore, the use of SLBs as substrate and the absence of liquid mixing within the liquid cell resulted in a slow diffusion of SbpA monomers to the solid-liquid interface, which lead to a depletion in SbpA concentration during S-layer growth. This depletion of the SbpA concentration at the solid-liquid interface limited the S-layer growth, even before competition with neighboring S-layer crystals became apparent.

Here we imaged S-layer self assembly on mica under continuous flow conditions to discover that both factors are markedly different. Depletion of the SbpA monomer concentration at the

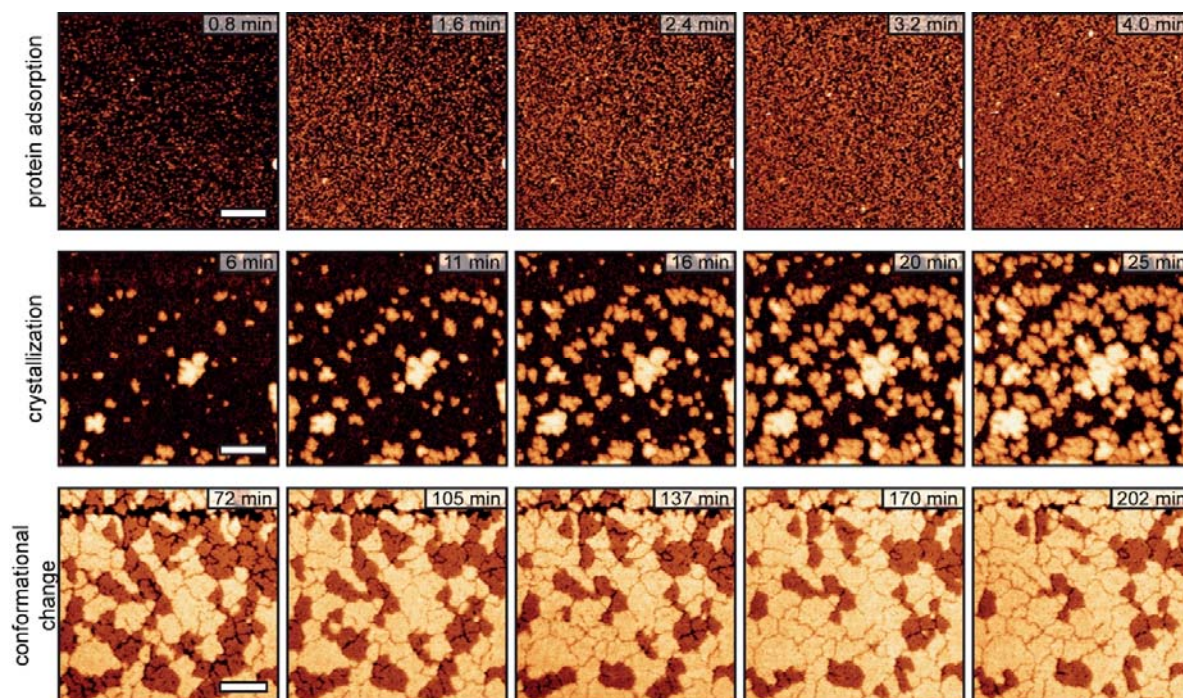


Figure 2 – Mica-liquid interface in the presence of SbpA at 50 $\mu\text{g/ml}$ imaged for over 8 h showing three distinct regimes: (I) 0.8 to 4 min: Protein adsorption taking place soon after introduction of SbpA into the solution, (II) 6 min to 25 min: Formation and growth of individual S-layer crystals until the surface is fully covered, and (III) 72 min to 202 min: Conformational transformations of the S-layer crystals. In (II), 2 different conformations can be noticed: low and high conformation. The low conformation transformed completely into the thermodynamically more stable high conformation after 4 h (III). On the top part of figures, it can be noticed the horizontal line intentionally scribed with the AFM tip to create a common positional marker. Scale bars: 400 nm.

mica-liquid interface has not been observed, i.e. R is constant. Furthermore, the growth of S-layer patches at the solid-liquid interface slows down when the mica surface becomes covered. The growth rate reaches zero once a full coverage is reached. This is included in the model by the term $(N_{T,m} - N_T)/N_{T,m}$ in Equation 1 (for a more detailed analysis of this term, the reader is referred to the supplementary information):

$$\frac{dN_T}{dt} = \sqrt{N_T} \cdot R \cdot \frac{N_{T,m} - N_T}{N_{T,m}} \quad 1$$

$$N_T(t) = N_{T,m} \cdot \tanh\left(\frac{R \cdot t}{2\sqrt{N_{T,m}}}\right)^2 \quad 1'$$

Here N_T is the number of tetrameric unit cells within the S-layer island, with $N_{T,m}$ the average number of unit cells at the point where the surface is fully covered. R is the tetramer attachment rate per unit cell along the borders of the existing S-layer islands.

Furthermore, S-layer nucleation has been observed well after existing S-layer crystals have started to grow, which is incorporated in the model by multiplying the perimeter driven growth term (Equation 1') by the number of S-layer crystals $N_{SL}(t)$.

Through careful consideration of the mechanism of S-layer self-assembly, as revealed by Figure , a model for the S-layer nucleation rate can be extracted. The number of S-layer islands depends both on the number of high density monomer globules, N_g , and on the rate constant, k_2 , for these globules undergo to relaxation into crystalline S-layers, i.e. $dN_{SL}/dt = N_g \cdot k_2$. In turn, the number of globules will increase over time, i.e. $N_g \equiv N_g(t)$. Although the time dependency of N_g is not exactly known, the most basic assumption that can be made is a linear approximation, i.e. $N_g(t) = k_1 \cdot t$. The fact that only a limited number of S-layer islands can fit within the measurement volume is included as a factor $(N_{SL,m} - N_{SL})/N_{SL,m}$ in Equation 2:

$$\frac{dN_{SL}}{dt} = k_1 \cdot k_2 \cdot t \cdot \frac{N_{SL,m} - N_{SL}}{N_{SL,m}} \quad 2$$

Thus, the number of S-layer islands over time is then described by:

$$N_{SL}(t) = N_{SL,m} \cdot \left(1 - e^{-\frac{k_1 \cdot k_2 \cdot (t-t_c)^2}{2 \cdot N_{SL,m}}}\right) \quad 2'$$

where N_{SL} is the total number of S-layer crystals at the mica surface, with $N_{SL,m}$ the maximum number that is reached when S-layer crystals fully cover the surface. t_c reflects the time it takes to form the first dense monomer globules (step I – protein adsorption in Figure). k_1 is the number of dense monomer globules that form per unit time (step II – crystallization in Figure). k_2 is the rate constant for dense monomer globules to

undergo relaxation into crystalline S-layers per unit time (step III – conformational change in Figure). Shin et al.¹⁹ found that during the conformational change of the S-layers, the coverage of the low conformation islands followed a simple exponential decay. This is considered by the model by multiplying of the total coverage by an expression for exponential decay:

$$A_{low}(t) = A_{tot} \cdot e^{-R_{conf} \cdot t} \quad 3$$

where A_{low} is the total area of the S-layer crystals in the low conformation and R_{conf} reflects the rate at which S-layers with low conformation relax to the high conformation.

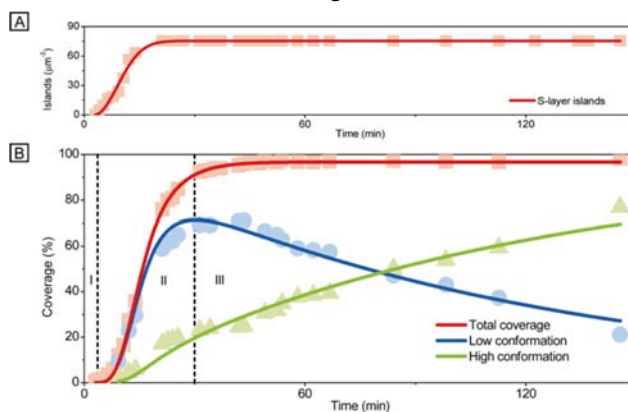


Figure 2 – Dynamical study of the self-assembly of SbpA protein at the mica-liquid interface. (a) The experimental data (fitted with the model shown in Equation 4) shows that S-layer islands only start to appear after a short period of time, as can be seen in Figure 2. After this, the number of S-layer islands start to increase faster over time, before reaching a steady state (full coverage). **(b)** The coverage of the S-layer islands tracked over time (red). A distinction is made between S-layer islands in a low (blue) or high (green) conformation. The experimental data for the total coverage is fitted with the mathematical model shown in Equation 4, the coverage of the low and high conformation is fitted with Equation 5 and 6, respectively. The 3 regimes, i.e. I, II and III, correspond to the three series of AFM images in Figure (protein adsorption, crystallization and conformational change).

Summarizing, the total area of S-layer crystals is obtained by combining equation 1' and 2' as follows:

$$A_{tot}(t) = N_{SL,m} \left(1 - e^{-\frac{k_1 \cdot k_2 \cdot (t-t_c)^2}{2 \cdot N_{SL,m}}}\right) \cdot N_{T,m} \cdot \tanh\left(\frac{R \cdot (t-t_c)}{2\sqrt{N_{T,m}}}\right)^2 \quad 4$$

and the total area of S-layers in the low and high conformation, are obtained from equations 5 and 6, respectively:

$$A_{low}(t) = N_{SL,m} \left(1 - e^{-\frac{k_1 \cdot k_2 \cdot (t-t_c)^2}{2 \cdot N_{SL,m}}}\right) \cdot N_{T,m} \cdot \tanh\left(\frac{R \cdot (t-t_c)}{2\sqrt{N_{T,m}}}\right)^2 \cdot (e^{-R_{conf} \cdot (t-t_c)}) \quad 5$$

$$A_{\text{high}}(t) = N_{\text{SL},m} \left(1 - e^{-\frac{k_1 \cdot k_2 \cdot (t-t_c)^2}{2 \cdot N_{\text{SL},m}}} \right) \cdot N_{T,m} \cdot \tanh \left(\frac{R \cdot (t-t_c)}{2 \sqrt{N_{T,m}}} \right)^2 \cdot (1 - e^{-R_{\text{conf}} \cdot (t-t_c)}) \quad 6$$

The models from Equations 4 to 6 were applied to the experimental data in Figure 3 by first fitting Equation 2' to the experimentally determined number of S-layer crystals per unit area. The parameters $N_{\text{SL},m}$, $k_1 \cdot k_2$ and t_c obtained from this fitting were then used as fixed input values in order to fit Equation 4 to the total coverage of S-layers over time. The two additional parameters $N_{T,m}$ and R obtained from this fit were then used as fixed input values to fit Equation 5 and 6 to the experimentally obtained values for the coverage of the low and high conformations, respectively. As shown in Figure 3, the models accurately fit the experimental data.

Regarding the on and off rates of the adsorbed proteins, once proteins bind to a growing island, they never leave. Hence, the off rate is zero. For this reason, we present a kinetic model, not one based on thermodynamic balance. With respect to the on and off rates of proteins to the surface from the solution, both rates are unknown. Previous studies have shown that the surface coverage is established during the initial exposure time to the solution prior to formation of the first nuclei. Afterwards, the adsorption rate to the surface is negligible compared to the binding rate to the islands.¹⁶ Consequently, the coverage on the surface drops to zero as the islands grow. The agreement of the observed behavior and the model predictions then imply that the off rate of adsorbed proteins from the surface is also negligible on the timescale of growth, but in fact, some desorption could occur without having any impact on the growth behavior of islands.

In summary, using dynamically resolved AFM data, we demonstrate that the self-assembly of S-layers can be separated into several processes, with distinct dynamics. The nucleation of S-layers follows an exponential growth law, the growth of existing S-layer crystals can be described by a perimeter driven growth model and the relaxation from a low conformation to a high conformation follows a simple exponential decaying function.

Furthermore, the high-resolution dynamic AFM data presented here shows the benefits of *in situ* high speed AFM with a continuous flow AFM setup. In this work, it has been shown with a single experiment how to resolve the dynamics of S-layer self-assembly at three vastly different time scales, that spans from seconds to hours and spatial scales, from nm to microns.

The robust experimental setup and thorough description of the dynamics of self-assembly may allow us to manipulate this process, thus controlling protein crystallization at the nanoscale.

Conflicts of interest

There are no conflicts of interest to declare.

Acknowledgements

Work at the Molecular Foundry was supported by the Office of Science, Office of Basic Energy Sciences, of the U.S. Department of Energy under Contract No. DE-AC02-05CH11231. We thank C. M. Ajo-Franklin for helpful discussions and feedback on this manuscript.

Notes and references

- U. B. Sleytr, in *International Review of Cytology*, ed. G. H. B. and J. F. Danielli, Academic Press, 1978, vol. 53, pp. 1–64.
- S.-V. Albers and B. H. Meyer, *Nat. Rev. Microbiol.*, 2011, **9**, 414–426.
- T. Pavkov-Keller, S. Howorka and W. Keller, in *Progress in Molecular Biology and Translational Science*, ed. S. Howorka, Academic Press, 2011, vol. 103, pp. 73–130.
- U. B. Sleytr and T. J. Beveridge, *Trends Microbiol.*, 1999, **7**, 253–260.
- R. P. Fagan and N. F. Fairweather, *Nat. Rev. Microbiol.*, 2014, **12**, 211–222.
- S. R. Hall, W. Shenton, H. Engelhardt and S. Mann, *ChemPhysChem*, 2001, **2**, 184–186.
- E. Györvary, A. Schroedter, D. V. Talapin, H. Weller, D. Pum and U. B. Sleytr, *J. Nanosci. Nanotechnol.*, 2004, **4**, 115–120.
- S. S. Mark, M. Bergkvist, X. Yang, L. M. Teixeira, P. Bhatnagar, E. R. Angert and C. A. Batt, *Langmuir*, 2006, **22**, 3763–3774.
- N. Ilk, C. Völlenkne, E. M. Egelseer, A. Breitwieser, U. B. Sleytr and M. Sára, *Appl. Environ. Microbiol.*, 2002, **68**, 3251–3260.
- P. Sampathkumar and M. L. Gilchrist, *Bioconjug. Chem.*, 2004, **15**, 685–693.
- J. Tang, A. Ebner, H. Badelt-Lichtblau, C. Völlenkne, C. Rankl, B. Kraxberger, M. Leitner, L. Wildling, H. J. Gruber, U. B. Sleytr, N. Ilk and P. Hinterdorfer, *Nano Lett.*, 2008, **8**, 4312–4319.
- X.-Y. Wang, D.-B. Wang, Z.-P. Zhang, L.-J. Bi, J.-B. Zhang, W. Ding and X.-E. Zhang, *Small*, 2015, **11**, 5826–5832.
- L. Velásquez and J. Dussan, *J. Hazard. Mater.*, 2009, **167**, 713–716.
- A. A. Makarova, E. V. Grachova, V. S. Neudachina, L. V. Yashina, A. Blüher, S. L. Molodtsov, M. Mertig, H. Ehrlich, V. K. Adamchuk, C. Laubschat and D. V. Vyalikh, *Sci. Rep.*, 2015, **5**, 8710.
- C. Xue, L. Zhang, R. Fan, S. Wang, H. Li, X. Luo, W. Liu and W. Song, *Eur. Food Res. Technol.*, 2014, **240**, 923–929.
- S. Chung, S.-H. Shin, C. R. Bertozzi and J. J. D. Yoreo, *Proc. Natl. Acad. Sci.*, 2010, **107**, 16536–16541.
- B. Rad, T. K. Haxton, A. Shon, S.-H. Shin, S. Whitelam and C. M. Ajo-Franklin, *ACS Nano*, 2015, **9**, 180–190.
- J. J. D. Yoreo and P. G. Vekilov, *Rev. Mineral. Geochem.*, 2003, **54**, 57–93.
- S.-H. Shin and S. Chung, *Proc. Natl. Acad. Sci.*, 2012, **109**, 12968–12973.
- B. Schuster, E. Györvary, D. Pum and U. B. Sleytr, *Methods Mol. Biol. Clifton NJ*, 2005, **300**, 101–123.

TOC

